Downlink channel tracking for FDD large-scale antenna systems

Downlink Channel Tracking for FDD Large-Scale Antenna Systems

Qi Liu*, Yu Han*, Fan Cao*, Jie Yang*, and Michail Matthaiou†
*National Mobile Communications Research Laboratory, Southeast University, Nanjing, China
†Institute of Electronics, Communications and Information Technology (ECIT), Queen's University Belfast, U.K.
Email: {qiliu, hanyu, cao.fan, yangjie}@seu.edu.cn, m.matthaiou@qub.ac.uk

***Abstract*— This paper tackles the problem of channel state information acquisition in mobile frequency-division-duplex large-scale antenna systems and proposes a novel low-complexity low-overhead method to track time-varying channels. Given the spatial reciprocity between uplink and downlink, the frequency-independent parameters are tracked from the uplink, greatly reducing the training and feedback overhead in the downlink. The uplink tracking method consists of two major modules. The first detection module works at the initial time instance to accurately estimate parameters by a comprehensive algorithm. Then, the second tracking module works at the subsequent instances to track the changes by utilizing a low-overhead algorithm as well as the parameters obtained at the previous instance. Especially, a simplified dictionary is further designed to decrease the computational complexity of the tracking module. Numerical results demonstrate that the proposed tracking method can successfully detect the newly occurred and disappeared paths, and accurately trace the changes of the time-varying channel.**

I. Introduction

The large-scale antenna technique has been widely employed in the coming fifth generation and future communication systems. Technologies to acquire Channel state information (CSI) keep being advanced and updated during the last few decades. Typically, coherent detection is utilized for CSI acquisition, which is usually obtained by pilot tones.

Many pilot-aided channel estimation methods have been proposed [1]–[4], which could be roughly divided into two categories, namely, nonparametric and parametric methods. In nonparametric methods, the CSI between each pair of antennas is directly estimated. In parametric methods, parameters of each path are estimated after the channel is characterized as a model such as the superposition of multiple paths [5]. Due to the large amount of pilots and feedback, nonparametric methods are hardly applied in frequency-division-duplex (FDD) large scale antanna systemS (LSASs), while parametric methods tackle this bottleneck. [6] and [7] utilize the Newtonized orthogonal matching pursuit (NOMP) method to extract parameters of each path in uplink and take advantage of the frequency-independent parameters obtained from the uplink to reconstruct the downlink channel. Another method for FDD three-dimensional (3D) Multi-Antenna Systems has been proposed in [8], which employs uniform planar array (UPA) at the BS and can estimate the downtilt and the azimuth. However, in time-varying channels, simply applying the NOMP algorithm at each time instance will cause unacceptably high computation complexity and large pilot overhead.

In this paper, we propose a time-varying downlink channel tracking method for FDD LSASs by utilizing the uplink-downlink spatial reciprocity. The method consists of two major modules, namely, an initial estimation module that works at the first time instance, and a low-complexity tracking module that traces the slow-changing channel parameters. Taking advantage of the strong coherence between two adjacent time instances, we can decrease the pilot overhead and computation complexity greatly when acquiring the current channel parameters by utilizing their previous estimates. Particularly, we simplify the codebook used in the NOMP algorithm to reduce the searching time. Numerical results show that the proposed tracking scheme can reconstruct the time-varying channel commendably with less run time and pilot overhead, and detect the disappearance and occurrence of the propagation paths acutely.

II. System Model

In a cell of the LSAS, the BS is located at the cell center and equipped with an $N_v \times N_h$ UPA, where N_v and N_h are the number of rows and columns, and the distances between two vertically adjacent antennas and two horizontally adjacent antennas are d_v and d_h, respectively. A single-antenna user moves at a speed of v and its initial distance to the BS is D. The LSAS works in FDD transmission mode. The uplink and downlink carrier frequencies are f_u and f_d, respectively. The OFDM module comprises of M subcarriers with spacing Δf.

With time going by, the channel varies with the change of user position. We focus on the channel in N_s time instances, and the duration between two instances is T_s. At the nth time instance, where $n = 1, \dots, N_s$, the uplink baseband channel across all BS antennas on subcarrier m is expressed as

$$\mathbf{h}_u(n,m) = \sum_{l=1}^{L(n)} g_{u,l}(n)\mathbf{a}^T\left(\varphi_l(n), \theta_l(n)\right) e^{j2\pi(m-1)\Delta f \tau_l(n)}, \quad (1)$$

where $m = 1, \dots, M$, $L(n)$ is the number of paths in the channel at the nth time instance, $g_{u,l}(n)$, $\varphi_l(n)$, $\theta_l(n)$, and $\tau_l(n)$ are the uplink complex gain, azimuth, downtilt, and delay of the lth path at the nth time instance, respectively. At the initial time, we set $L(1) = \bar{L}$. For the lth path, $g_{u,l}(1) \sim \mathcal{CN}(0,1)$, $\theta(1)$ and $\varphi(1)$ are both randomly generated from $[0, 2\pi)$, and $\tau_l(1)$ is randomly chosen from $[0, 1/(\Delta f)]$. The changes of these parameters are modeled as Markov processes.

At the nth time instance where $n > 1$, new occurrence and disappearance of paths may happen, i.e.,

$$L(n) = \begin{cases} L(n-1)+1, & \text{occurrence}, \\ L(n-1)-1, & \text{disappearance}, \\ L(n-1), & \text{else}. \end{cases} \quad (2)$$

The complex gain satisfies

$$g_{u,l}(n) = g_{u,l}(n-1)(1+\gamma_g(n)\nu_{g,\max}), \quad (3)$$

where $\gamma_g(n)$ is a ratio factor arbitrarily chosen from [-1,1], and $\nu_{g,\max} \in [0,1]$ is the maximum change ratio which depends on the user's speed. Similarly, we describe the changes of azimuth, downtilt, and delay based on their maximum change amounts:

$$\begin{aligned} \tau_l(n) &= \tau_l(n-1) + \Delta\tau_{\max}\gamma_\tau(n), \\ \theta_l(n) &= \theta_l(n-1) + \Delta\theta_{\max}\gamma_\theta(n), \\ \varphi_l(n) &= \varphi_l(n-1) + \Delta\varphi_{\max}\gamma_\varphi(n), \end{aligned} \quad (4)$$

where

$$\Delta\tau_{\max} = \frac{vT_s}{c} \quad (5)$$

happens when the moving direction of the user is along the propagation path,

$$\Delta\theta_{\max} = \Delta\varphi_{\max} = 2\arctan\left(\frac{vT_s}{2D}\right) \quad (6)$$

happen when the path is line-of-sight and the moving direction is vertically and horizontally orthogonal to the path, respectively, and $\gamma_\tau(n)$, $\gamma_\theta(n)$, and $\gamma_\varphi(n)$ are ratio factors that are randomly drawn from $[-1,1]$. The N_vN_h-dimensional vector $\mathbf{a}(\varphi,\theta)$ denotes the steering vector of the UPA, which is written as

$$\mathbf{a}(\varphi,\theta) = \mathbf{a}_v(\theta) \otimes \mathbf{a}_h(\varphi,\theta), \quad (7)$$

where

$$\mathbf{a}_v(\theta) = \left[1, e^{j2\pi\frac{d_v}{\lambda}\sin\theta}, \cdots, e^{j(N_v-1)2\pi\frac{d_v}{\lambda}\sin\theta}\right], \quad (8)$$

and

$$\mathbf{a}_h(\varphi,\theta) = \left[1, e^{j2\pi\frac{d_h}{\lambda}\cos\theta\sin\varphi}, \cdots, e^{j(N_h-1)2\pi\frac{d_h}{\lambda}\cos\theta\sin\varphi}\right]. \quad (9)$$

Given the spatial reciprocity between uplink and downlink, $L(n)$, $\varphi_l(n)$, $\theta_l(n)$, and $\tau_l(n)$ hold frequency-independency and are identical in uplink and downlink. We suppose the uplink baseband as 0 Hz. Then, the downlink baseband channel on the mth subcarrier is

$$\mathbf{h}_d(n,m) = \sum_{l=1}^{L(n)} g_{d,l}(n)\mathbf{a}\left(\theta_l(n),\varphi_l(n)\right)e^{j2\pi(f_d-f_u+(m-1)\Delta f)\tau_l(n)}, \quad (10)$$

where $g_{d,l}(n)$ is the complex downlink gain of the lth path at time instance n that has the same Markov feature with $g_{u,l}(n)$.

In this paper, we aim to track the time-varying downlink channel for the FDD LSAS to obtain the channel on all subcarriers and time instances, i.e., $\mathbf{h}_d(n,m)$ for $m = 1,\dots,M$ and $n = 1,\dots,N_s$. According to [8], the downlink channel at a time instance can be reconstructed using the frequency-independent parameters extracted from the uplink and the estimated downlink complex gains. Therefore, we utilize frequency-independency as well. At time instance n, we first estimate $\varphi_l(n)$, $\theta_l(n)$, and $\tau_l(n)$ for $l = 1,\dots,L(n)$, and then estimate $g_{d,l}(n)$. The approach to acquire the downlink complex gains is similar to [8] and omitted here. In this paper, we focus on tracing the frequency-independent parameters from the uplink.

III. Tracing Frequency-Independent Parameters

Given that the BS has no knowledge about the moving speed of the user, we should insert pilots frequently to trace the change of the frequency-independent parameters in order to overcome the worst high-speed case. Hence, the typical value of T_s is small, and the change amounts of parameters are not large. The received uplink all-one pilot at the nth time instance across all BS antennas and subcarriers is expressed as

$$\mathbf{y}(n) = \sum_{l=1}^{L(n)} g_{ul}(n)\mathbf{a}\left(\varphi_l(n),\theta_l(n)\right) \otimes \mathbf{p}(\tau_l(n)) + \mathbf{z}_u, \quad (11)$$

where

$$\mathbf{p}(\tau) = \left[1, e^{j2\pi\Delta f\tau(n)}, \cdots, e^{j2\pi(M-1)\Delta f\tau(n)}\right], \quad (12)$$

$\mathbf{z}_u$ is the additive noise vector, and each element of $\mathbf{z}_u$ is independent and identically distributed (i.i.d.) with zero mean and unit variance. Considering the slow variance of the tracing targets, this section proposes a low-complexity scheme to trace the frequency-independent parameters based on their previous tracing results. This scheme consists of two major modules, namely, an initial estimation module that works at the first time instance and a low-complexity tracking module that operates at the following time instances.

1) Initial Estimation Module: At the first time instance, no priori CSI is available. We apply the NOMP algorithm [8] on $\mathbf{y}(1)$ to accurately extract the parameters of each path. NOMP algorithm is a combination of orthogonal matching pursuit (OMP) algorithm and Newton method. The OMP algorithm firstly makes a rough estimation of the signal, and obtains the initial parameters of each path. After the parameters of the lth path are obtained by OMP algorithm, the parameters of this path are refined by Newton method. Afterward, the Newton method is applied on each previously estimated path to cyclicly refinement all the estimates, further improving the accuracy. The final estimation results in the initial time instance are denoted as $\mathbf{P}_1 = \{\hat{\varphi}_l(1), \hat{\theta}_l(1), \hat{\tau}_l(1)\}_{l=1,\dots,\hat{L}(1)}$.

2) Low-Complexity Tracking Module: If the estimation accuracy of the $(n-1)$th instance is sufficient, where $n > 1$, then in the nth instance, we can take advantage of the results of the previous instance to decrease the complexity of estimation. The channel parameters change slightly between two time instances. Thanks to this feature, we propose a low-complexity tracking module that consists of checking, tracing and new path estimation steps. The checking step functions as a detector which decides whether the estimates at the $(n-1)$th instance could be fully utilized. The tracing step re-estimates the parameters in the nth instance on the basis of those in the $(n-1)$th instance. When a new path occurs, the tracking module will enter into the new path estimation step, which uses the NOMP algorithm to estimate the parameters of the new path. We then introduce the three steps in detail.

Step 1. Checking: If the variations of the delays and angles are tiny, we can reuse these values and compensate their changes through re-estimating the gains. To achieve this, we first use the least square (LS) method to estimate the uplink gains as

$$\hat{\mathbf{g}}_u(n) = (\mathbf{A}^H(n-1)\mathbf{A}(n-1))^{-1}\mathbf{A}^H(n-1)\mathbf{y}(n), \quad (13)$$

where

$$\mathbf{A}(n-1) = [\mathbf{A}_1(n-1), \cdots, \mathbf{A}_{\hat{L}(n-1)}(n-1)] \quad (14)$$

is the coefficient matrix with

$$\mathbf{A}_l(n-1) = \mathbf{a}^T(\hat{\varphi}_l(n-1), \hat{\theta}_l(n-1)) \otimes \mathbf{p}^T(\hat{\tau}_l(n-1)). \quad (15)$$

Then we check if the updated gains can compensate the changes by utilizing the stopping threshold δ of the NOMP iterations [8]. We calculate the residual of signal by

$$\mathbf{y}_r(n) = \mathbf{y}(n) - \mathbf{A}(n-1)\hat{\mathbf{g}}_u(n). \quad (16)$$

If the residual power is below the threshold, i.e.,

$$\|\mathcal{F}\{\mathbf{y}_r(n)\}\|_\infty^2 < \delta = \ln(N_v N_h M) - \ln(-\ln(1-P_{fa})), \quad (17)$$

where $P_{fa} \in [0,1]$ is the false alarm rate, then the parameters of the $(n-1)$th instance can still be utilized in the nth instance, and the tracking module ends with $\mathbf{P}_n = \mathbf{P}_{n-1} = \{\hat{\varphi}_l(n-1), \hat{\theta}_l(n-1), \hat{\tau}_l(n-1)\}_{l=1,\ldots,\hat{L}(n-1)}$.

Step 2. Tracing: If the residual power $\|\mathcal{F}\{\mathbf{y}_r(n)\}\|_\infty^2$ is higher than the threshold δ, which means the results in the $(n-1)$th instance cannot be directly applied to the nth instance, then we perform tracing on each path to re-estimate its delay and angles, where $\mathcal{F}\{\cdot\}$ represents taking Fourier transformation and $\|\cdot\|_\infty$ denotes the infinite norm. We still refer to the NOMP algorithm, but simplify the dictionary in the OMP steps. The complexity of the OMP step is directly decided by the size of the dictionary. Decreasing the size of the dictionary further reduces the complexity of the tracing step. The key to simplify dictionary in the nth instance is to utilize the estimation result of the $(n-1)$th instance. Assume that the $\hat{L}(n-1)$ paths are arranged in the decreasing order of the amplitude of the gain. Since the amplitude of the gain does not change significantly, we design the dictionary $\mathbf{C}_l(n)$ for the lth path as

$$\mathbf{C}_l(n) = \mathbf{C}_l^{angle}(n) \otimes \mathbf{C}_l^{\tau}(n), \quad (18)$$

where the definition of the angle sub-dictionary $\mathbf{C}_l^{angle}(n)$ of the lth path at time instance n can be seen in (19), and the delay sub-dictionary is defined as

$$\mathbf{C}_l^{\tau}(n) = \exp\left\{j2\pi[0,\ldots,M-1]^T \Delta f \mathbf{\Gamma}_l(n)\right\}, \quad (20)$$

where R_v, R_h, and R_τ are the oversampling rates of the downtilt, azimuth, and delay, respectively. β_v, β_h, β_τ denote the compressing times of the ranges of downtilt, azimuth, and delay, respectively. We perform the OMP step with the simplified dictionary to coarsely estimate the parameters of each path. Select the codeword in the dictionary that has the maximum inner product with $\mathbf{y}_{r,l-1}(n)$, where

$$\mathbf{y}_{r,l-1}(n) = \mathbf{y}(n) - \sum_{i=1}^{l-1} \hat{\hat{g}}_{u,i}(n)\mathbf{A}_i(n), \quad (21)$$

$\hat{\hat{g}}_{u,i}(n)$ is the updated uplink gain of the ith path,

$$\mathbf{A}_i(n) = \mathbf{a}^T(\hat{\hat{\varphi}}_i(n), \hat{\hat{\theta}}_i(n)) \otimes \mathbf{p}^T(\hat{\hat{\tau}}_i(n)), \quad (22)$$

and $\hat{\hat{\varphi}}_i(n)$, $\hat{\hat{\theta}}_i(n)$, and $\hat{\hat{\tau}}_i(n)$ are the updated downtilt, azimuth, and delay, respectively. The coarse estimates of the lth path are the parameters of the selected codeword. Afterwards, the Newton method is first applied on each path to refine the estimates, and then cyclicly on the estimates all the first l paths to further reduce the residual. After re-estimating the parameters of the lth path, we then check whether this path disappears by comparing $\mathbf{y}_{r,l-1}(n)$ and $\mathbf{y}_{r,l}(n)$. If $\|\mathcal{F}\{\mathbf{y}_{r,l-1}(n)\}\|_\infty^2 \leq \|\mathcal{F}\{\mathbf{y}_{r,l}(n)\}\|_\infty^2$, then the lth path is considered to vanish, and the residual is $\mathbf{y}_{r,l-1}(n)$. Till now, the trace of the lth path ends, and we turn to the $(l+1)$th path. After tracing all the $\hat{L}(n-1)$ paths, we obtain $\mathbf{P}_n = \{\hat{\hat{\varphi}}_l(n), \hat{\hat{\theta}}_l(n), \hat{\hat{\tau}}_l(n)\}_{l=1,\ldots,\hat{\hat{L}}(n)}$, where $\hat{\hat{L}}(n)$ is

$$\mathbf{C}_l^{angle}(n) = \exp\left\{j2\pi[0,1,\ldots,N_v-1]^T \frac{d_v}{\lambda} \sin\mathbf{\Theta}_l(n)\right\} \otimes \exp\left\{j2\pi[0,1,\ldots,N_h-1]^T \frac{d_h}{\lambda} \cos\mathbf{\Theta}_l(n) \sin\mathbf{\Phi}_l(n)\right\} \quad (19)$$

$$\begin{aligned}
\mathbf{\Theta}_l(n) &= \left[\hat{\theta}_l(n-1) - \frac{\pi}{\beta_v}, \ldots, \hat{\theta}_l(n-1) - \frac{\pi}{R_v N_v}, \hat{\theta}_l(n-1), \hat{\theta}_l(n-1) + \frac{\pi}{R_v N_v}, \ldots, \hat{\theta}_l(n-1) + \frac{\pi}{\beta_v}\right] \\
\mathbf{\Phi}_l(n) &= \left[\hat{\varphi}_l(n-1) - \frac{\pi}{\beta_h}, \ldots, \hat{\varphi}_l(n-1) - \frac{\pi}{R_h N_h}, \hat{\varphi}_l(n-1), \hat{\varphi}_l(n-1) + \frac{\pi}{R_h N_h}, \ldots, \hat{\varphi}_l(n-1) + \frac{\pi}{\beta_h}\right] \quad (20) \\
\mathbf{\Gamma}_l(n) &= \left[\hat{\tau}_l(n-1) - \frac{1}{\beta_\tau \Delta f}, \ldots, \hat{\tau}_l(n-1) - \frac{1}{R_\tau M \Delta f}, \hat{\tau}_l(n-1), \hat{\tau}_l(n-1) + \frac{1}{R_\tau M \Delta f}, \ldots, \hat{\tau}_l(n-1) + \frac{1}{\beta_\tau \Delta f}\right]
\end{aligned}$$

the number of remained paths. If the residual $\mathbf{y}_{r,\hat{\hat{L}}(n)}(n)$ is less than the threshold δ, the estimation is considered to end here. Otherwise, we consider a new path occurs and the tracking module turns to Step 3.

Step 3. New path estimation: If a new path is generated, we must detect it and estimate its downtilt, azimuth, and delay with no prior information about them. Keeping the tracing results of existing paths, we apply the NOMP algorithm directly on the residual $\mathbf{y}_{r,\hat{\hat{L}}(n)}(n)$ to detect the new paths. Step 3 ends till the reduced residual is below δ. The new detections are denoted as $\{\hat{\varphi}_j(n), \hat{\theta}_j(n), \hat{\tau}_l(n)\}_{j=1,\ldots,\Delta L(n)}$, where $\Delta L(n)$ is the number of newly appeared paths, and the final results of Step 3 are $\mathbf{P}_n = \mathbf{P}_n \cup \{\hat{\varphi}_j(n), \hat{\theta}_j(n), \hat{\tau}_l(n)\}_{j=1,\ldots,\Delta L(n)}$.

We summarize the working steps of the tracking module in **Algorithm 1**. After obtaining the parameters of the uplink channel, we can use these parameters to reconstruct the downlink channel. Since the uplink and downlink channels share the same physical propagation path, the delays and the angles of the uplink and downlink channels are the same. With frequency-independent parameters estimated from the uplink, i.e., $\mathbf{P}_n$, the downlink gains at time instance n can be calculated using a limited amount of downlink training and feedback overhead. Then, the BS can successfully reconstruct the downlink channel at time instance n by applying the parameters in (1).

Algorithm 1: Tracking algorithm

Input: Uplink pilot received in the nth instance $\mathbf{y}(n)$, and estimates in the $(n-1)$th instance $\mathbf{P}_{n-1} = \{\hat{\varphi}_l(n-1), \hat{\theta}_l(n-1), \hat{\tau}_l(n-1)\}_{l=1,\ldots,\hat{L}(n-1)}$
Output: Estimates in the nth instance $\mathbf{P}_n$
Initialization: $l = 0, \mathbf{y}_r(n) = \mathbf{y}(n), \mathbf{P}_n = \{\}$;
Calculate $\hat{\mathbf{g}}_u(n)$;
Update $\mathbf{y}_r(n) = \mathbf{y}(n) - \mathbf{A}(n-1)\hat{\mathbf{g}}_u(n)$;
if $\|\mathcal{F}\{\mathbf{y}_r(n)\}\|_\infty^2 < \delta$ **then**
  $\mathbf{P}_n = \mathbf{P}_{n-1}$
  break;
else
  for $l = 1 \to \hat{L}(n-1)$ **do**
    Coarsely estimate the parameters of the lth path.
    Apply Newton step on the coarse estimates.
    Cyclicly apply Newton step on the estimates of all the first l paths and obtain $\{\hat{\hat{\varphi}}_l(n), \hat{\hat{\theta}}_l(n), \hat{\hat{\tau}}_l(n)\}_{l=1,\ldots,l}$
    Update the residual $y_{r,l}(n)$
    if $\|\mathcal{F}\{\mathbf{y}_{r,l-1}(n)\}\|_\infty^2 \leq \|\mathcal{F}\{\mathbf{y}_{r,l}(n)\}\|_\infty^2$ **then**
      Exclude $\hat{\hat{\varphi}}_l(n), \hat{\hat{\theta}}_l(n), \hat{\hat{\tau}}_l(n)$;
      $\mathbf{y}_r(l) = \mathbf{y}_r(l-1)$;
      continue;
    end
  end
  if $\|\mathcal{F}\{\mathbf{y}_{r,\hat{\hat{L}}(n)}(n)\}\|_\infty^2 < \delta$ **then**
    $\mathbf{P}_n = \{\hat{\hat{\varphi}}_l(n), \hat{\hat{\theta}}_l(n), \hat{\hat{\tau}}_l(n)\}_{l=1,\ldots,\hat{\hat{L}}(n)}$;
    break;
  else
    Apply NOMP algorithm to $\mathbf{y}_r(\hat{L}(n))$ and obtain $\{\hat{\varphi}_j(n), \hat{\theta}_j(n), \hat{\tau}_l(n)\}_{j=1,\ldots,\Delta L(n)}$;
    $\mathbf{P}_n = \mathbf{P}_n \cup \{\hat{\varphi}_j(n), \hat{\theta}_j(n), \hat{\tau}_l(n)\}_{j=1,\ldots,\Delta L(n)}$
  end
end

IV. Numerical results

The theoretical settings for observing the estimated performance of the NOMP algorithm are shown in Table I. We take 50 times of Monte Carlo simulations with $N_s = 5$ at each time. At the initial instance, there are 6 paths. Then, the numbers of paths at the subsequent instances will randomly increase or decrease with a probability of 3%.

Fig. 1 shows the real and estimated angles at the initial and the 2nd instances, respectively. The red stars represent the estimates derived by the NOMP algorithm in the initial instance, and the blue stars represent the results of the proposed tracking scheme at the second time instance. As is shown in Fig. 1(a), the number of paths has increased from 6 to 7. It can be seen that the tracking algorithm can detect the newly added path with a low normalized mean square error of 0.01. Fig. 1(b) shows the scene where the 6th path disappears. The simulation demostrates that when the 5th path is estimated, the residual energy is already less than the threshold. At this point, the algorithm ends the iteration, and the disappeared path is successfully excluded from the estimates.

Fig. 2 illustrates the mean-squared errors (MSEs) of different algorithms. The abscissa represents the indices of 5 time instances in each Monte Carlo simulation, and the ordinate represents the MSE performance at these 5 time instances. The MSE of the reconstructed channel is defined as

$$\text{MSE} = \mathbb{E}\left\{\frac{\|\hat{\mathbf{h}} - \mathbf{h}\|^2}{\|\mathbf{h}\|^2}\right\}. \tag{23}$$

The "linear minimum mean square error (LMMSE)" curve represents the average MSE of the downlink channel over 50 times of simulations by the LMMSE method, which functions as a baseline of the performance of our proposed method. The "tracking (1)" curve indicates the performance of the proposed tracking method at one simulation time. As is shown in this curve, the MSE performance of the tracking scheme at the 2nd instance is as well as that of the initial instance estimated by NOMP algorithm. The MSE performance of the 3rd instance is slightly worse, because the amount of changes on parameters are small and the updated residual is still below the threshold. Then, the tracking method ends at the checking step. Although the MSE performance of the 3rd instance is slightly degraded, the result is still much better than the LMMSE method, and the accuracy of this estimation is perfectly acceptable as well. The "tracking (mean)" and "NOMP (mean)" curve are the average of the downlink channel reconstruction over 50 times of simulations with half of the amount of pilots used by the original NOMP algorithm. The two curves show that our proposed method has the same performance with the NOMP algorithm but requires fewer pilots.

Notably, the dictionary sizes of NOMP algorithm and tracking algorithm for each path are 172800 and 2700, respectively. Thus, our proposed method can achieve the same performance as the original NOMP algorithm in time-varying channel with much less complexity and pilot overhead.

TABLE I: Parameter settings

System layout	
Parameter	Values
N_v / N_h	8 / 8
M	300
Δf	75 kHz
$f_d - f_u$	300 MHz
N_s	5
T_s	5 ms
$\Delta\varphi_{\max}$ / $\Delta\theta_{\max}$ / $\Delta\tau_{\max}$	0.05 / 0.05 / 0.003
Algorithm settings	
Parameter	Values
P_{fa}	0.01
β_v / β_h / β_τ	2 / 2 / 3
R_v / R_h / R_τ	3 / 3 / 2
Monte-carlo times	50

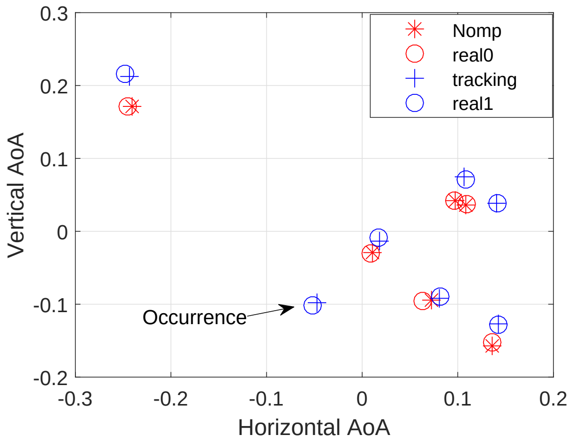

(a) The occurance of path

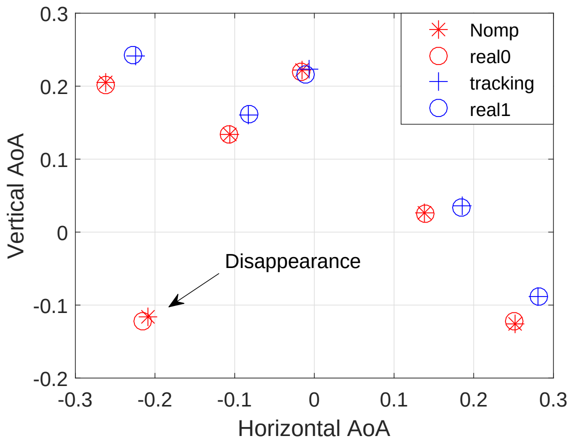

(b) The disappearance of path

Fig. 1: Accuracy of the proposed tracking method and the NOMP algorithm. The tracking algorithm can detect the occurrence and disappranace of paths accurately.

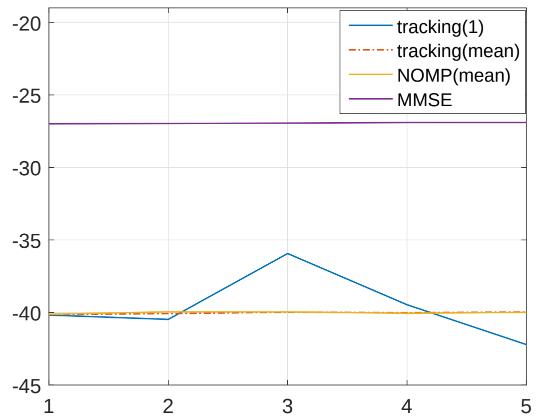

Fig. 2: MSE performance of the NOMP and the tracking algorithms. The tracking algorithm can reach comparable performance as NOMP algorithm with much fewer pilots.

V. Conclusion

In this paper, a novel time-varying downlink channel tracking method was proposed for the FDD LSAS. A simplified dictionary and a novel scheme was designed to decrease the computation complexity. This tracking method consists of two major modules. In the first detection module, we estimate the uplink channel at the initial time instance by NOMP algorithm. In the second tracking module at the subsequent instances, we track the channel by using the parameters from the previous instance. Then, the downlink channel gains were recalculated and fed back by applying a small amount of overhead. The downlink channel at each time instance was reconstructed by the uplink-estimated frequency-independent parameters and the downlink gains. Simulation results showed that with less runtime and pilot overhead, the proposed tracking scheme can reconstruct the time-varying channel feasibly.

References

[1] G. Z. Karabulut, A. Yongacoglu, "Estimation of Time-Varying Channels with Orthogonal Matching Pursuit Algorith," *Symp. Adv. Wired Wireless Comm.*, pp. 141-144, 2005.

[2] A. Adhikary, J. Nam, J. Ahn, and G. Caire, "Joint spatial division and multiplexing: The large-scale array regime," *IEEE Trans. Inf. Theory, vol.*, 59, no. 10, pp. 6441-6463, Oct. 2013.

[3] X. Dong, W. Lu. "Linear interpolation in pilot symbol assisted channel estimation for OFDM," *IEEE Trans. Wirel. Commun.*, vol. 6, no. 5, pp. 1910-1920, May 2007.

[4] B. Mamandipoor, D. Ramasamy, and U. Madhow, "Newtonized orthogonal matching pursuit: Frequency estimation over the continuum," *IEEE Trans. Signal Process.*, vol. 64, no. 19, pp. 5066-5081, Oct. 2016.

[5] Z. Gao, L. Dai, Z. Wang, and S. Chen,"Spatially common sparsity based adaptive channel estimation and feedback for FDD massive MIMO," *IEEE Trans. Signal Process.*, vol. 63, no. 23, pp. 6169-6183, Dec. 2015.

[6] Y. Han, Q. Liu, C.-K. Wen, "FDD massive MIMO based on efficient downlink channel reconstruction," arXiv preprint arXiv:1902.06174, 2019.

[7] Y. Han, T. H. Hsu, C.-K. Wen, " Efficient downlink channel reconstruction for FDD transmission systems," *in Proc. 27th WOCC*, pp. 1-5, 2018.

[8] Q. Liu, Y. Han, C.-K. Wen, and S. Jin, "Downlink Channel Reconstruction for FDD 3D Multi-Antenna Systems," in *Proc. 24th IEEE APCC*, pp. 1-6, Nov. 2018.